Korean J. Chem. Eng., 40(5), 1228-1233 (2023)
DOI: 10.1007/s11814-022-1336-4

pISSN: 0256-1115
eISSN: 1975-7220

Light-reflective properties of spherical TiO_2 particles coated with (3-aminopropyl)trimethoxysilane, chitosan, SiO_2, and SnO_2

Hani Ko and Seog Woo Rhee†

Department of Chemistry, Kongju National University, Gongjudaehak-ro 56, Gongju 32588, Korea
(*Received 23 July 2022 • Revised 19 October 2022 • Accepted 6 November 2022*)

Abstract−We synthesized TiO_2-based composite pigment materials and investigated their light reflection properties. Micrometer-sized spherical TiO_2 particles were synthesized by the sol-gel method using hydrolysis and condensation reactions of the precursors, and the rutile phase was prepared by calcining at 800 °C. TiO_2-based composite materials were synthesized by coating the surface of the calcined TiO_2 with (3-aminopropyl)trimethoxysilane (APTMS), chitosan, SiO_2, and SnO_2. The morphologies of the composite materials were characterized by field emission scanning electron microscopy (FE-SEM), and the structural properties of the composite materials were identified using powder X-ray diffraction (PXRD) analysis. Finally, the light reflection properties were investigated by measuring the percent reflectance in the wavelength range 300-2,500 nm of the composite materials by diffuse-reflectance UV-Vis-NIR spectroscopic analysis. In the wavelength range 300-2,500 nm, the composite materials showed solar reflectance of 86-93%. The composite materials synthesized in this study have potential for use as heat reflective pigment materials.

Keywords: Light Reflection, TiO_2, Core/Shell, Composite, Sol-gel Method

INTRODUCTION

Titanium dioxide generally exists as one of the polymorphs: rutile, anatase, and brookite [1]. TiO_2 in the rutile phase is thermodynamically the most stable [2], and has high density due to its structurally dense atomic arrangement (compared to the anatase phase). It also has efficient light scattering and light reflection properties. Therefore, it has been used as a light-reflecting material for ultraviolet and infrared light for a long time [3,4]. TiO_2 in the anatase phase has high photoactivity, so it is used as a photocatalyst and in dye-sensitized solar cells [5-8]. TiO_2 in the brookite phase is in a metastable state, and relatively few studies have been conducted because it is difficult to prepare as a pure single phase [9].

Because the light scattering and light reflection qualities vary depending on the size of a particle, the applied wavelength range varies according to the size and shape of a TiO_2 particle [10-12]. When light is radiated onto solid particles, symmetrical spherical particles cause single scattering, whereas particles with anisotropic shapes, such as rods, triangular prisms, or cubes, cause multiple scattering in the spectral region of visible light [13].

Titanium dioxide, when used as a white pigment for paints, must be designed to cause maximum scattering in the Mie region [10], so it is manufactured as particles of size 200-300 nm, which is about 0.5 times the wavelength (360-780 nm) of the visible light region. Titanium dioxide used for blocking ultraviolet light has a particle size of 60-120 nm to show maximum reflectance in the harmful ultraviolet region (100-360 nm), whereas titanium dioxide for reflecting infrared light (780-2,500 nm) has a particle size of about 1,000 nm to reflect near-infrared light efficiently [10].

Because TiO_2 used as a white pigment exhibits extreme photocatalytic properties in the presence of ultraviolet light, it is necessary to modify the surface of TiO_2 with organic or inorganic materials [14,15]. In general, this has been done by coating the surface of TiO_2 with SiO_2 or Al_2O_3 [16,17]. Wei et al. studied the change of photocatalytic activity of TiO_2 particles coated with various transition metal oxides [15]. Wu et al. proposed a method of synthesizing TiO_2 particles coated with hydrated alumina while protecting the photocatalytically active TiO_2 from surface exposure [18].

A study on the near-infrared reflectance of composite materials coated with TiO_2 particles on the surface of a mineral, such as mica, which is very commonly used as an additive in paints, was carried out. Gao et al. synthesized nanocomposite materials by attaching nanoparticles having a rutile TiO_2 structure to the mica surface. The light reflection characteristics were investigated by measuring the reflectance between 400 and 2,500 nm for the materials [19]. Mica has a plate-like structure and is widely used as a paint additive. Therefore, when composite materials are synthesized by applying a rutile TiO_2 structure to the surface of the mica, it is possible to use composite materials that maintain the plate-like structure of mica and have the light reflection property of TiO_2.

In this study, spherical TiO_2 particles were synthesized using a general sol-gel synthesis method, and core/shell composite materials were prepared by applying APTMS, chitosan, SiO_2, and SnO_2 to the surfaces of TiO_2 particles. APTMS forms a self-assembled monolayer on the surface of TiO_2 particles to change the surface charge and is used to improve the dispersibility of particles in a solvent. Chitosan is used to enhance the antibacterial activity of TiO_2 particles. The insulator SiO_2 is used to lower the photocatalytic activity of TiO_2 particles, and the semiconductor SnO_2 is used to enhance the photocatalytic activity. Finally, the light reflection ability of the

†To whom correspondence should be addressed.
E-mail: jisanrhee@kongju.ac.kr

composite materials was investigated.

EXPERIMENTAL

1. Reagents and Materials

All chemicals were purchased from Sigma-Aldrich Chemical Co. (USA), Junsei Chemical Co. (Japan) and Samchun Pure Chemical Co., LTD. (Korea). They were of reagent grade and used without further purification.

2. Synthesis of Spherical Rutile Phase TiO_2

Spherical TiO_2 was synthesized using a method reported in the literature [20]. To a 500 mL round-bottom flask, 200 mL of ethanol, 1.2 mL of DI water, and 1.2 mL of 0.4 mM KCl aqueous solution were added and stirred until completely dissolved. A precursor solution of 100 mL of ethanol and 5.6 mL of tetrabutylorthotitanate (TBOT, 16.5 mmol) was added to the solution at a rate of 4 mL/min using a dropping funnel, followed by further stirring at room temperature for 6 h. The reaction mixture was centrifuged (4,000 rpm, 10 min) to separate a solid product, and the sediment was washed with ethanol five times and dried at 60 °C for 24 h. The dried sample was calcined at 800 °C for 3 h to obtain spherical rutile phase TiO_2.

3. Surface Modification of TiO_2 by APTMS

To a 250 mL beaker, 1 g of calcined TiO_2, 20 mL of ethanol, and 100 mL of DI water were added, and the mixture was dispersed by ultrasonication for 30 min. To the mixture, 0.02 mL of APTMS was added, and then, the mixture was stirred at 500 rpm for 35 min. The reaction mixture was centrifuged (4,000 rpm, 5 min) to separate a solid product, and the sediment was washed with ethanol four times and then dried at 60 °C for 24 h.

4. Synthesis of Chitosan@TiO_2

To a 100 mL beaker, 0.5 g of calcined TiO_2 and 25 mL of DI water were added, and the mixture was dispersed by ultrasonication for 30 min. The mixture was added to a solution prepared by mixing 1.4 mL of acetic acid, 25 mL of DI water and 1 g of chitosan. Then, the mixture was stirred at 500 rpm for 10 min. The reaction mixture was centrifuged (4,000 rpm, 5 min) to separate the solid product, and the sediment was washed five times (once with DI water, once with 0.1 M aqueous NaOH solution, and three times with DI water) and then dried at 60 °C for 24 h.

5. Synthesis of SiO_2@TiO_2

To a 250 mL beaker, 1 g of calcined TiO_2 and 50 mL ethanol were added, and the mixture was dispersed by ultrasonication for 30 min. To the mixture, 35 mL of ethanol and 15 mL of aqueous NH_3 solution (15 M) were added. Then, a solution of 100 mL of ethanol and 0.35 mL of tetraethylorthosilicate (TEOS) was added at a rate of 4 mL/min using a dropping funnel, while being stirred at 500 rpm at room temperature for 3 h. The reaction mixture was centrifuged (4,000 rpm, 5 min) to separate a solid product, and the sediment was washed with ethanol four times and dried at 60 °C for 24 h.

6. Synthesis of SnO_2@TiO_2

To a 100 mL round-bottom flask, 195 mg of $SnCl_4$ (0.75 mmol) and 15 mL of ethanol were added, and then stirred at 60 °C for 2 h until completely dissolved. To the solution, 3.5 g of citric acid (18 mmol) and 2 mL of ethylene glycol (36 mmol) were added. The solution was further stirred for 3 h to obtain a $SnCl_4$/ethanol precursor solution. To a 250 mL round-bottom flask, 0.5 g of calcined TiO_2 and 60 mL of DI water were added, sonicated, and refluxed at 90 °C for 40 min. To the mixture, 15 mL of $SnCl_4$/ethanol precursor solution was added at a rate of 0.2 mL/min using a dropping funnel. It was then stirred for another 18 h. The reaction mixture was centrifuged (4,000 rpm, 10 min) to separate a solid product, and the sediment was washed with ethanol four times and dried at 60 °C for 24 h. The dried solid material was calcined at 800 °C for 3 h to obtain SnO_2@TiO_2.

7. Characterization

The morphologies of the synthetic solid materials were analyzed using field emission scanning electron microscopy (HR FE-SEM) images. These were obtained from Pt-coated samples at an accelerating voltage of 30 kV with a Tescan MIRA3-LMH scanning electron microscope (Czechia). Powder X-ray diffraction (XRD) patterns were recorded on a Rigaku MiniFlex-II diffractometer (Japan) using Cu Kα radiation (λ=0.1543 nm) at 4 kV and 35 mA, a scan rate of 2θ=4°/min and range 2θ=20-80°. The thermal decomposition and phase transition of the amorphous TiO_2 were monitored by thermogravimetric analysis (TGA) and differential scanning calorimetry (DSC) using a Q600 SDT (TA Instruments, USA) thermal analyzer under nitrogen gas with a ramp speed of 10 °C/min and a temperature range of 25-900 °C. Using a diffuse-reflectance UV/Vis/NIR spectrometer (UV-3600, Shimadzu, Japan) equipped with an integrating sphere (ISR-3100, Shimadzu), the percent reflectance of each composite material was measured in the range 300-2,500 nm. Spectralon (Lapsphere Inc., USA), which is prepared by compressing Teflon, was used as a reference material.

RESULTS AND DISCUSSION

1. Synthesis

In an ethanol solution containing water, tetrabutylorthotitanate reacts with water to hydrolyze, and spherical particles are formed by the condensation reaction of the hydrolyzed titanate. The factors affecting the particle size are the concentration of the TBOT solution, reaction temperature, addition rate, and the stirring rate. In this study, the experimental conditions were optimized to synthesize TiO_2 particles of 1 μm. The aminosilane [(3-aminopropyl)trimethoxysilane] reacts with Ti-OH functional groups present on the surface of TiO_2 to form Ti-O-Si covalent bonds. As a result, a self-assembled monolayer of APTMS is formed on the surface of TiO_2. Chitosan is soluble in acidic solution because it has -NH_2 functional groups, but is insoluble in basic solution. Because the viscosity of an acidic solution of chitosan is very high, it very well coats the surface of TiO_2 particles. By washing the obtained composite material with aqueous NaOH solution, TiO_2 particles with chitosan shells were prepared. In an ethanol solution containing water, tetraethylorthosilicate also reacts with water to hydrolyze, and shells are formed on the surface of TiO_2 by the condensation reaction of the hydrolyzed silicate. In ethanol solution, $SnCl_4$ forms a sol state and a solvolysis reaction occurs. Shells were formed on the surface of TiO_2 by the condensation reaction of the sol. Pure SnO_2 shells were obtained by calcining a gel-coated solid sample at 800 °C to remove organic matter and hydroxide ions.

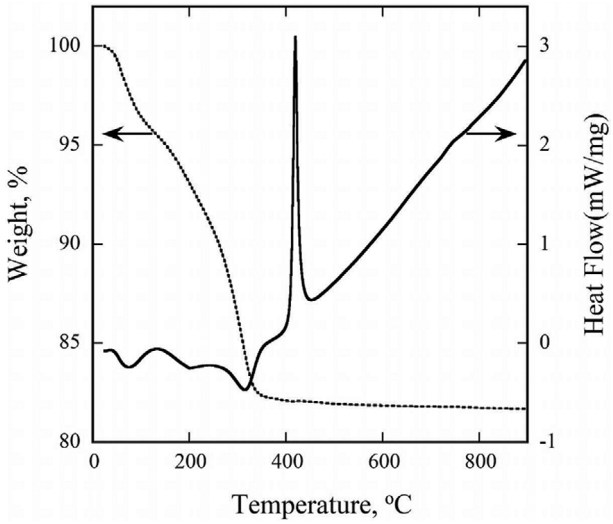

Fig. 1. TGA and DSC analyses of as-synthesized TiO_2.

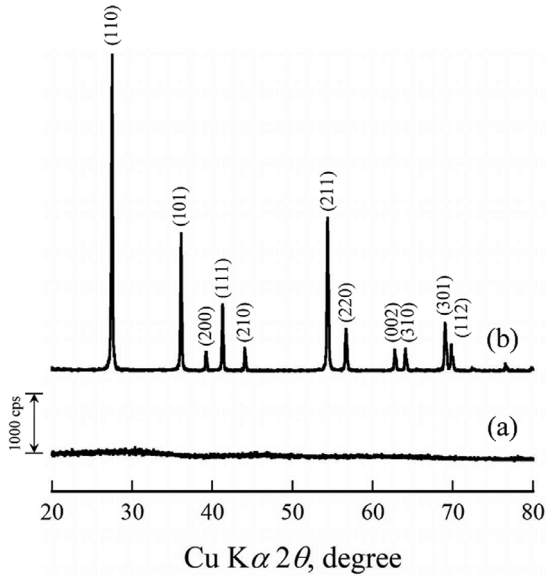

Fig. 2. Powder X-ray diffraction patterns of TiO_2: (a) As-synthesized TiO_2 and (b) TiO_2 calcined at 800 °C.

2. Synthesized TiO_2 and Calcined TiO_2

TiO_2 synthesized by the sol-gel method contains undecomposed metal alkoxide, metal hydroxide, and residual solvent. Thermal analysis thermograms (TGA and DSC) of the synthesized TiO_2 are shown in Fig. 1. The endothermic process centered at 76.3 °C in the temperature range 25-133 °C is due to the release of ethanol used as a solvent [21], and the mass lost is 4.5%. The endothermic process centered at 315 °C in the temperature range 133-375 °C is caused by the release of organic substances and water due to thermal decomposition of metal alkoxide and metal hydroxide [21]. The mass loss in this process is about 13.3%. The exothermic process occurring at 420 °C is due to the phase transition of amorphous synthetic TiO_2 to the anatase phase [21]. The exothermic process centered at at 741 °C occurs because of the phase transition from the anatase phase to the rutile phase [21]. Therefore, TiO_2 calcined at 800 °C or higher temperature has a pure rutile phase.

Fig. 2 shows the powder XRD patterns of the synthesized TiO_2 and the calcined TiO_2. TiO_2 synthesized by the sol-gel method has no crystallinity and shows very broad XRD patterns, so a clear phase cannot be identified. TiO_2 calcined at 800 °C for 3 h shows distinct diffraction lines at 2θ=27.5° (110), 36.1° (101), 39.2° (200), 41.3° (111) and 44.1° (210). This is consistent with TiO_2 with a rutile phase, as reported in the literature (JCPDS card No. 78-1510). Moreover, because TiO_2 peaks with anatase phase were not observed, the calcined TiO_2 is pure rutile phase.

Fig. 3 shows the SEM images of the synthesized TiO_2 and the calcined TiO_2. The synthesized TiO_2 particles (Fig. 3(a)) are spherical and have a smooth surface. The average particle size is about 970 nm. The TiO_2 particles (Fig. 3(b)) calcined at 800 °C show an approximately spherical shape, but the surface is not as smooth with the amorphous TiO_2 particles. Small grains that form as amorphous TiO_2 undergo a phase transition to rutile phase through the anatase phase, and appear to agglomerate to form large aggregates during the calcination process. The grain boundaries are clearly distinguishable in the SEM image.

3. TiO_2-based Core/Shell Composite Materials

Fig. 4 shows SEM images of TiO_2-based core/shell composite

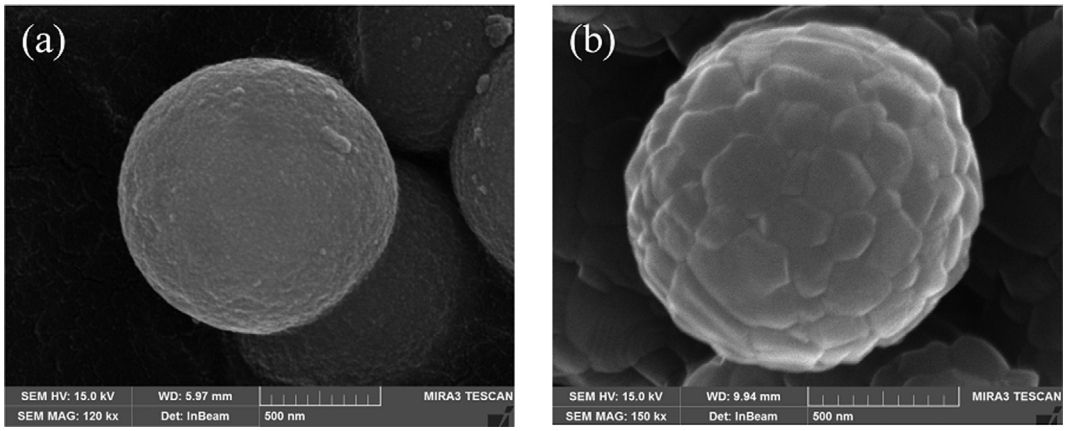

Fig. 3. HR FE-SEM images of TiO_2: (a) As-synthesized TiO_2 and (b) TiO_2 calcined at 800 °C.

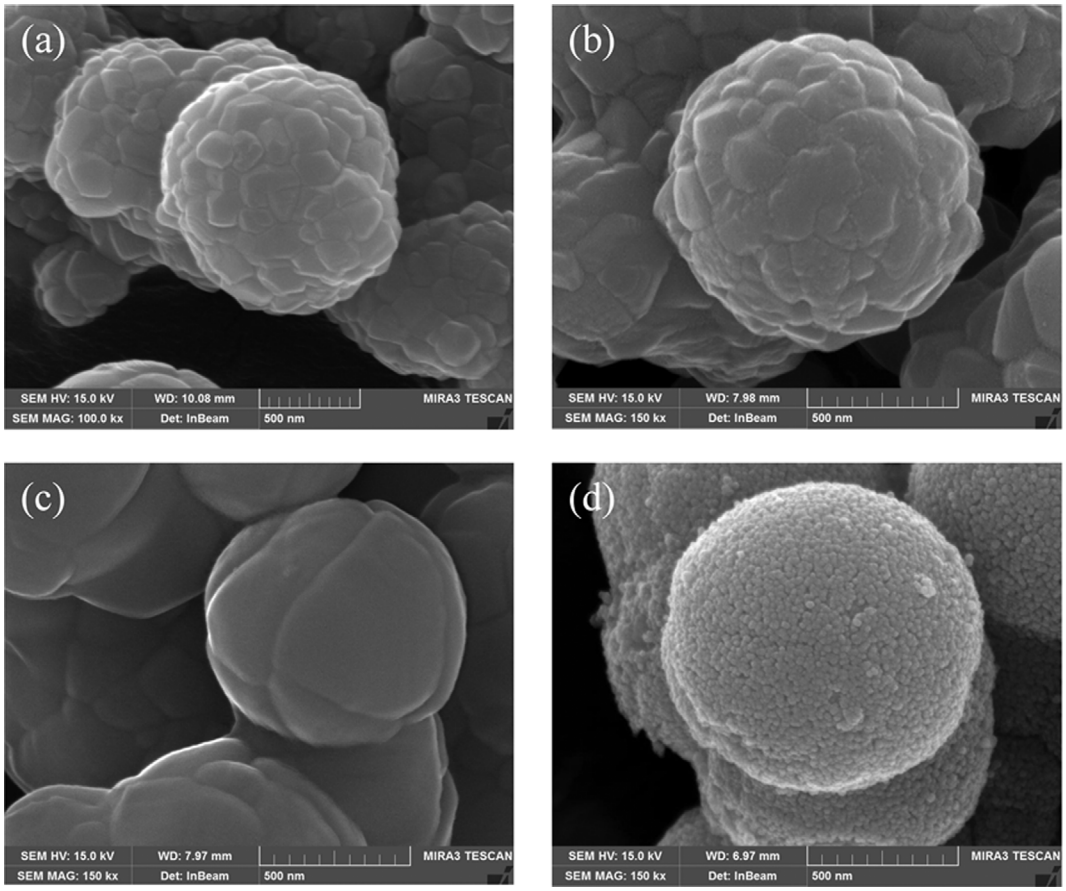

Fig. 4. HR FE-SEM images of core/shell composite materials: (a) APTMS coated TiO_2, (b) chitosan@TiO_2, (c) SiO_2@TiO_2, and (d) SnO_2@TiO_2.

materials. Because APTMS forms a self-assembled monolayer on the surface, TiO_2 coated with APTMS (Fig. 4(a)) has a shape similar to that of a calcined TiO_2 particle. In the case of chitosan@TiO_2 (Fig. 4(b)), the shape of the particles is similar to that of calcined TiO_2, but a very thin film of chitosan, a biopolymer, can be observed on the surface of the core TiO_2 particle. In the case of SiO_2@TiO_2 (Fig. 4(c)), the shape of the particles is slightly different from that of calcined TiO_2. A uniformly thin film of SiO_2 is formed on the surface of TiO_2 particles, and the thickness of the shell as measured through the SiO_2 shell partially peeled from the particle surface of SiO_2@TiO_2 is about 20 nm (data not shown). In the case of SnO_2@TiO_2 (Fig. 4(d)), SnO_2 with an average size of about 30 nm was uniformly coated on the surface of TiO_2, and the shape of the composite material is close to spherical.

Fig. 5 shows the powder XRD patterns of the TiO_2-base core/shell composite materials. All TiO_2-based composites with core/shell structures show distinct diffraction patterns due to rutile phase TiO_2 like calcined TiO_2. This means that the structure of the rutile phase is maintained during the synthesis process. Because chitosan@TiO_2 and APTMS-coated TiO_2 are both coated with organic materials, there is no crystalline phase, so only the TiO_2 pattern is observed in the XRD pattern. Because SiO_2 is not crystalline, SiO_2@TiO_2 shows only the XRD pattern of TiO_2. SnO_2@TiO_2 shows not only the pattern of TiO_2 but also the new diffraction pattern of SnO_2 with rutile structure (JCPDS card No. 41-1445) at 2θ=26.8° (110), 34.1° (101), 38.2° (200), and 52.0° (211).

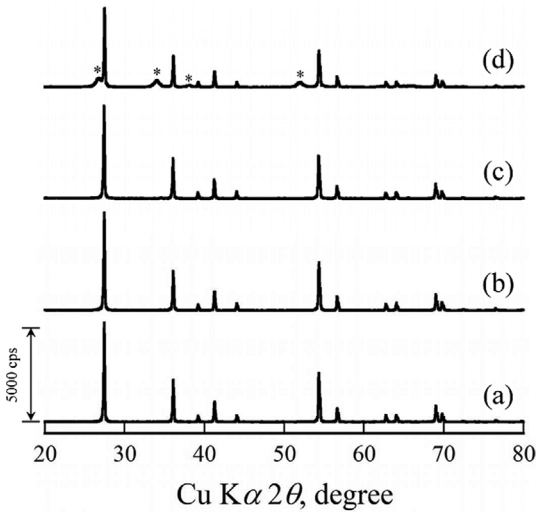

Fig. 5. Powder X-ray diffraction patterns of core/shell composite materials: (a) APTMS coated TiO_2, (b) chitosan@TiO_2, (c) SiO_2@TiO_2, and (d) SnO_2@TiO_2. The diffractions of SnO_2 are indicated by *.

4. Light Reflective Properties of Composite Materials

Fig. 6 shows the diffuse-reflectance spectra of synthesized TiO_2

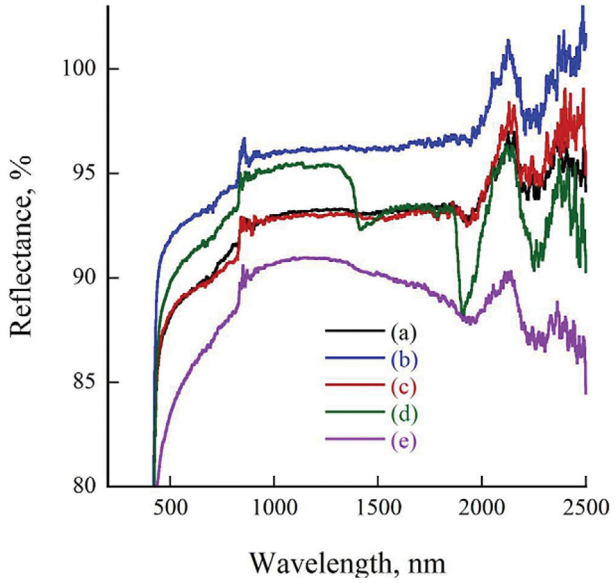

Fig. 6. Diffuse-reflectance spectra of (a) TiO_2 calcined at 800 °C, (b) APTMS coated TiO_2, (c) chitosan@TiO_2, (d) SiO_2@TiO_2, and (e) SnO_2@TiO_2.

Table 1. Solar reflectance data of core/shell composite materials. Spectralon was used as a reference material

Sample	Solar reflectance, *R* (%)		
	300-2,500 nm	300-780 nm	780-2,500 nm
TiO_2	89.9	84.4	93.3
APTMS-TiO_2	93.1	87.8	96.5
Chitosan@TiO_2	89.9	84.4	93.3
SiO_2@TiO_2	91.1	85.7	94.5
SnO_2@TiO_2	86.4	80.7	89.9

and core/shell composite materials in the UV/Vis/NIR region. Table 1 provides the solar reflectance, *R* (%), in the visible region and near-infrared region. In the case of TiO_2, the solar reflectance is 89.9% in the wavelength range 300-2,500 nm, 84.4% in the visible region, and 93.3% in the near-infrared region. The weak absorption peak at 1,907 nm is an overtone peak [22] caused by the vibration of water molecules and OH groups on the TiO_2 surface. The solar reflectance in the infrared region is similar to the value of 96.0% reported in the literature [23]. In the 300-2,500 nm region, the solar reflectance (93.1%) of APTMS-coated TiO_2 was observed to be higher than that of TiO_2 and chitosan@TiO_2 showed a solar reflectance (89.9%) very similar to that of TiO_2. So even if a very thin film of organic molecule, or biopolymer is coated onto the surface of the TiO_2 particle, the light reflection ability of the TiO_2 particle is not significantly affected. It seems that the two materials show similar solar reflectance because they consist of calcined TiO_2 cores of the same size with a rutile phase as shown in the XRD patterns and SEM images. In the case of SiO_2@TiO_2, the solar reflectance (91.1%) of SiO_2@TiO_2 was slightly higher than that of TiO_2. However, strong overtone peaks caused by vibration of OH groups are observed at 1,415 nm and 1,907 nm in the IR region because the SiO_2 synthesized using this method is a porous material that contains many OH groups on the surface [22]. In the case of SnO_2@TiO_2, the solar reflectance (86.4%) was slightly lower than that of TiO_2, because the 30 nm SnO_2 coated on the TiO_2 surface is an *n*-type semiconductor [24] that forms a small number of surface charge carriers that absorb some of the irradiated light.

CONCLUSIONS

Core/shell composite materials were synthesized by coating the surface of micrometer-sized spherical TiO_2 particles with organic/inorganic materials. Then, the light reflection ability of these materials was investigated. The core material, TiO_2, was made in the form of spherical particles through hydrolysis and condensation of the precursor material, and was finally calcined at 800 °C. The methods used to synthesize core/shell composite materials in this work are very simple, inexpensive and useful. The surface-treated TiO_2 composite materials showed solar reflectance similar to that of TiO_2, the core material, in the UV-Vis-NIR region. In particular, the solar reflectance of the composite materials in the NIR region was 93-97%. TiO_2-based core/shell composite materials coated using non-conductive materials with excellent solar reflectance could be used as paint pigments to reflect radiated heat.

ACKNOWLEDGEMENTS

This work was supported by a research grant from Kongju National University in 2020.

REFERENCES

1. M. Landmann, E. Rauls and W. G. Schmidt, *J. Phys.: Condens. Matter.*, **24**, 195503 (2012).
2. Y. Kumari, L. K. Jangir, A. Kumar, M. Kumar and K. Awasthi, *Solid State Commun.*, **263**, 1 (2017).
3. P. Jeevanandam, R. S. Mulukutla, M. Phillips, S. Chaudhuri, L. E. Erickson and K. Klabunde, *J. Phys. Chem. C*, **111**, 1912 (2007).
4. H. Lu, M. Huang, K.-S. Shen, J. Zhang, S.-Q. Xia, C. Dong, Z.-G. Xiong, T. Zhu, D.-P. Wu, B. Zhang and X.-Z. Zhang, *Nanoscale Res. Lett.*, **13**, 328 (2018).
5. J. Panpranot, K. Kontapakdee and P. Praserthdam, *J. Phys. Chem. B*, **110**, 8019 (2006).
6. V. Gowthambabu, M. Deshpande, R. Govindaraj, V. K. N. Krishna, M. L. Charumathi, J. M. Kumar, M. S. D. Vignesh, R. I. Daniel and P. Ramasamy, *J. Mater. Sci.: Mater. Electron.*, **32**, 26306 (2021).
7. S. H. Pak, J. H. Park and C. G. Park, *Korean J. Chem. Eng.*, **39**, 1863 (2022).
8. Y. Zhang, W. Jiang, Y. Ren, B. Wang, Y. Liu, Q. Hua and J. Tang, *Korean J. Chem. Eng.*, **37**, 536 (2020).
9. L. Sang, Y. Zhao and C. Burda, *Chem. Rev.*, **114**, 9283 (2014).
10. Y. Matsuo, *New developments of high-reflective materials*, pp. 3-12, CMC, Tokyo, Japan (2010).
11. V. A. Vlasov, A. L. Astafyev and A. N. Zarubin, *IOP Conf. Ser.: Mater. Sci. Eng.*, **81**, 012087 (2015).
12. W. E. Vargas, *J. Appl. Phys.*, **88**, 4079 (2000).
13. R. Ragheb and U. Nobbmann, *Sci. Rep.*, **10**, 21768 (2020).

14. H. Zhou, S. Sun and H. Ding, *Adv. Mater. Sci. Eng.*, **2017**, 9562612 (2017).
15. B.-X. Wei, L. Zhao, T.-J. Wang, H. Gao, H.-X. Wu and Y. Jin, *Adv. Powder Technol.*, **24**, 708 (2013).
16. O. K. Park and Y. S. Kang, *Colloids Surf. A: Physicochem. Eng. Aspects*, **257-258**, 261 (2005).
17. Y. S. Zhang, Y. M. Liu, C. Ge, H. B. Yin, M. Ren, A. L. Wang, H. Feng, J. Chen, T. S. Jiang and L. B. Yu, *Powder Technol.*, **192**, 171 (2009).
18. H.-X. Wu, T.-J. Wang and Y. Jin, *Ind. Eng. Chem. Res.*, **45**, 5274 (2006).
19. Q. Gao, X. Wu and Y. Fan, *Dyes Pigm.*, **109**, 90 (2014).
20. H. Liu, X. Dong, X. Wang, C. Sun, J. Li and Z. Zhu, *Chem. Eng. J.*, **230**, 279 (2013).
21. T. He, X. Guo, K. Zhang, Y. Feng and X. Wang, *RSC Adv.*, **4**, 5880 (2014).
22. E. Finocchio, I. Baccini, C. Cristiani, G. Dotelli, P. G. Stampino and L. Zampori, *J. Phys. Chem. A*, **115**, 7484 (2011).
23. T. Thongkanluang, N. Chirakanphaisarn and P. Limsuwan, *Procedia Eng.*, **32**, 895 (2012).
24. H. Bendjedidi, A. Attaf, H. Saidi, M. S. Aida, S. Semmari, A. Bouhdjar and Y. Benkhetta, *J. Semicond.*, **36** 123002 (2015).